INVESTIGATION ON ANTIPROLIFERATIVE MECHANISMS OF *ALSTONIA ANGUSTILOBA*-SILVER NANOPARTICLES IN SKIN SQUAMOUS CELL CARCINOMA

NURHIDAYAH BINTI AB RAHIM

UNIVERSITI SAINS MALAYSIA

2023

INVESTIGATION ON ANTIPROLIFERATIVE MECHANISMS OF *ALSTONIA ANGUSTILOBA*-SILVER NANOPARTICLES IN SKIN SQUAMOUS CELL CARCINOMA

by

NURHIDAYAH BINTI AB RAHIM

Thesis submitted in fulfilment of the requirements
for the degree of
Doctor of Philosophy

August 2023

ACKNOWLEDGEMENT

Alhamdulillah, all praises are only to Allah; may He bestow His blessings and peace onto our dear prophet Muhammad S.A.W., as well as his family and associates. With perseverance and sincerity, I am able to exert considerable effort and strength to complete my research.

First and foremost, I would like to express my heartfelt gratitude and appreciation to my supervisor, Associate Professor Dr Md. Azman Seeni Mohamed and , my co-supervisors, Ts. Dr Rabiatul Basria S. M. N. Mydin for their unwavering support, encouragement, and developmental advice throughout my research.

My deepest gratitude to Mr Zulkapli Ibrahim of Rimba Ilmu Botanic Garden, Universiti Malaya, for kindly providing the plant's leaves and all staff of Centralise Research Laboratory 3 (CRL-3), Advanced Medical and Dental Institute (AMDI), Universiti Sains Malaysia for their assistance in providing their services and facilities for my studies. I also thank all staff in CRL-1 for allowing and helping me to use their equipment, such as the fluorescence microscope and flow cytometer.

I express my gratitude to all my lab mates (Imah, Zafirah, Sarah, Munirah, Wan Amira, Julia, Rohanizah, Hock Ing, Hidayah Sabri, Masyitah and many more) for their abundant assistance and support, especially throughout the most challenging parts of this project.

Last but not least, special thanks to my husband (Mohd Hafiz Mail), my parents (Ab. Rahim Ab. Wahid and Alimah Omar), and children (Aakif, Aarisya and Aarif) and families for their love, support, understanding and encouragement.

TABLE OF CONTENTS

LIST OF TABLES

Page

LIST OF FIGURES

Page

LIST OF SYMBOLS AND ABBREVIATIONS

%	percentage
$	dollar
≤	less than or equal to
>	more than
°C	degree celcius
=	equal to
°	degree
2θ	2 theta
±	plus minus
-	minus
A. angustiloba	*Alstonia angustiloba*
A. angustiloba-AgNPs	*Alstonia angustiloba*-silver nanoparticles
A. pneumatophora	*Alstonia pneumatophora*
A. scholaris	*Alstonia scholaris*
A431 cell line	skin squamous cell carcinoma
A549 cancer cell	adenocarcinomic human alveolar basal epithelial cells
Ag	silver
Ag^{+}	silver ion
Ag^{0}	silver (zero state)
$AgNO_3$	silver nitrate
AgNPs	silver nanoparticles
AJCC	American Joint Committee on Cancer
AK	actinic keratoses
ALA	5-aminolevulinic acid
$AlCl_3$	aluminium chloride
ANOVA	one-way analysis of variance
AO	acridine orange
AO/PI	acridine orange/ propidium iodide
Apaf-1	apoptotic protease activating factor 1
APS	ammonium persulfate
ATCC	American Type Culture Collection

ATP	adenosine triphosphate
Bax	Bcl-2 Associated X-protein
BCC	basal cell carcinoma
Bcl-2	B-cell lymphoma-2
BD Biosciences	Becton-Dickson Biosciences
BSA	bovine serum albumin
BWH	Brigham and Women's Hospital
C	cell concentration
C=C	alkenes
Ca^{2+}	calcium ion
$CaCl_2$	calcium chloride
CARD	caspase-recruitment domains
CDKs	cyclin-dependent kinases
cells/mL	cells per mililitre
CHK1	checkpoint kinase 1
CHK2	checkpoint kinase 2
CIP/KIP	CDK interacting protein/Kinase inhibitory protein
Cl	chloride
cm	centrimetre
cm^{-1}	reciprocal centimetres
CO_2	carbon dioxide
cSCC	cutaneous squamous cell carcinoma
CVD	chemical vapour deposition
D	average crystallite size
DAPI	4′,6-diamidino-2-phenylindole
DCM	dichloromethane
DCM:MeOH	dichloromethane:methanol
DED	death effector domains
Df	dilution factor
DLS	dynamic light scattering
DMEM	Dulbecco's modified eagle medium
DMSO	dimethyl sulfoxide
DNA	deoxyribonucleic acid
DPPH	2,2-diphenyl-1-picrylhydrazyl

DR3	death receptor 3
E&C	electrodesiccation and curettage
E2F	E2 transcription factor
EC_{50}	median effective concentration
ECL	ECL
EDTA	ethylenediaminetetraacetic acid
EGFR	epidermal growth factor receptor
ESI	electrospray ionisation
FADD	fas associated death domain
FBS	fetal bovine serum
FESEM	field emission scanning electron microscopy
FITC	fluorescein isothiocyanate
FITC/PI	fluorescein isothiocyante/ propidium iodide
FT-IR	Fourier transform infrared spectroscopy
g	gram
G1	gap phase
G2	second gap phase
h	hour(s)
HCl	hydrochloric acid
HCT-15	human colorectal carcinoma
HeLa	cervical cancer cells
HEPES/NaOH	4-(2-hydroxyethyl)-1-piperazineethanesulfonic acid/ sodium hydroxide
Hf	haemacytometer factor
HPV	human papillomavirus
HRP-linked antibody	horseradish peroxidase-linked antibody
I Gy	grey
IARC	International Agency for Research on Cancer
IC_{50}	half-maximal inhibitory concentration
IFN-χ	interferon-χ
IgG	immunoglobulin G
IL-1	interleukin-1
IL-18	interleukin-18
INK4	inhibitor of CDK4
INOR	Nano Optoelectronics Research and Technology

Ipharm	Malaysian Institute of Pharmaceuticals and Nutraceuticals
ISO	International Organization for Standardization
JCPDS	Joint Committee on Powder Diffraction Standards
KB cell line	human epithelial carcinoma cells
KBr	potassium bromide
KCl	potassium chloride
keV	kiloelectron volt
KIP	kinase-inhibitory protein
kV	kilovolt
L	litre
L/min	litre/minute
L929 cell line	mouse fibroblast
LC	liquid chromatography
LC-MS	liquid chromatography-mass spectrometry
M	mitosis phase
M	molar
m/z	mass-to-charge ratio
mA	milliampere
MCF-7	human breast cancer (hormone dependant)
MDA-MB-231	human breast cancer (hormone independant)
MeOH	methanol
mg	miligrams
mg GAE/g	total gallic acid equivalents per g extract
mg QE/g	total quercetin equivalents per gram of extract
mg/mL	milligrams per mililitre
min	minute(s)
mL	millilitre
mL/min	mililitre per minute
mm	milimetre
mM	millimolar
MMP-2	matrix metalloproteinase-2
MMS	Mohs micrographic surgery
mol/L	moles per liter
MOMP	mitochondrial outer membrane permeabilisation

MS	mass spectrometry
MS/MS	tandem mass spectrometry
MTS	3-(4,5-dimethylthiazol-2-yl)-5-(3-carboxymethoxyphenyl)-2-(4-sulfophenyl) 2Htetrazolium
MTT	3-(4, 5-dimethylthiazolyl-2)-2, 5-diphenyl-tetrazolium bromide
mV	millivolt
N_2H_4	hydrazine
$NaBH_4$	sodium borohydride
NaCl	sodium chloride
$NaHCO_3$	sodium carbonate
NCCN	National Comprehensive Cancer Network
NER	nucleotide excision repair
NF-κB	nuclear factor kappa-light-chain-enhancer of activated B cells
nm	nanometre
NMSC	non-melanoma skin cancer
O	oxygen
OD	optical density
–OH	hydroxyl
p53	a type of tumor suppressor gene
PA1 cancer cells	human ovarian cancer
PARP	Poly ADP (Adenosine Diphosphate)-Ribose Polymerase
PBS	phosphate-buffered saline
PCNA	proliferating cell nuclear antigen
PDT	photodynamic therapy
pH	potential of hydrogen
PI	propidium iodide
PLK1	Polo-like kinase 1
ppm	parts per million
PPPM	per patient per month
psi	pounds of force per square inch of area
PVP	polyvinyl pyrrolidine
Q	quadrant counted
Q-TOF	quadrupole time of flight
R^2	R-squared

RB	retinoblastoma protein
RIPA buffer	radioimmunoprecipitation assay buffer
RNA	ribonucleic acid
ROS	reactive oxygen species
rpm	revolutions per minute
S	synthesis phase
SCC	squamous cell carcinoma
SCCI	invasive squamous cell carcinoma
SCCIS	Bowen's disease
SCCIS	Squamous cell carcinoma in situ
SD	standard deviation
SDS	sodium dodecyl sulfate
SEM	standard error of mean
SEM-EDX	scanning electron microscopy-energy dispersive X-ray analysis
SMO	mutation of smoothened
SPR	surface plasmon resonance
tBid	truncated Bid
TBS	tris-buffered saline
TEM	transmission electron microscopy
TEMED	tetramethylethylenediamine
TFC	total flavonoid content
TNF	tumour necrosis factor
TNF-R1	umor necrosis factor receptor t
TPC	total phenolic content
TRAIL-R1	tumour necrosis factor-related apoptosis-inducing ligand-receptor 1
TRAIL-R2	tumour necrosis factor-related apoptosis-inducing ligand-receptor 2
U/mL	units per mililitre
UICC	Union for International Cancer Control
UK	United Kingdom
US FDA	United States Food and Drug Administration
USA	United States of America
USD	United States Dollar
USM	Universiti Sains Malaysia

UV	ultraviolet
UVA	ultraviolet A
UVB	ultraviolet B
UVC	ultraviolet C
UVR	ultraviolet radiation
UV–Vis	ultraviolet-visible
V	volt
VCap	capillary voltage
VDR	vitamin D receptor
VEGF	vascular endothelial growth factor
w/v	weight per volume
WHO	World Health Organization
WST-1	sodium 5-(2,4-disulfophenyl)-2-(4-iodophenyl)-3-(4-nitrophenyl)-2Htetrazolium
XP	Xeroderma pigmentosum
XRD	X-ray diffraction
XTT	sodium 2,3-bis(2-methoxy-4-nitro-5-sulfophenyl)-5-[(phenylamino)-carbonyl]-2H-tetrazolium
β	the full width at half maximum (FWHM)
β-Actin	beta actin
β-ME	2-mercaptoethanol
θ	the diffraction angle
λ	the X-ray wavelength
μg/mL	micrograms per milliliter
μL	microlitre
μm	micrometre

LIST OF APPENDICES

KAJIAN MEKANISME ANTIPROLIFERASI *ALSTONIA ANGUSTILOBA*- NANOPARTIKEL PERAK TERHADAP SEL KARSINOMA SKUAMOS KULIT

ABSTRAK

Kaedah tradisional sintesis nanopartikel yang lazimnya menggunakan bahan kimia toksik dan tenaga cukup besar berkemungkinan menjejaskan alam sekitar dan kesihatan manusia. Baru-baru ini, sintesis nanopartikel berasaskan tumbuhan (AgNPs) telah muncul sebagai kaedah sintesis hijau yang mempunyai harapan untuk berjaya. Dalam tesis ini, sintesis hijau AgNPs yang menggunakan ekstrak akueus daun *A. angustiloba* dilaporkan. Mekanisme antiproliferatifnya turut dinilai. Pada mulanya, sifat fisiokimia *A. angustiloba*-AgNPs dicirikan menggunakan spektrofotometri UV-Vis, FT-IR, FESEM, EDX, TEM, XRD dan penganalisis saiz partikel *(zetasizer*). Kesitotoksikan *A. angustiloba*-AgNPs telah diperiksa melalui assai MTT terhadap titisan sel kanser A431. Morfologi sel dirawat telah diperiksa melalui mikroskopi pendarfluor dan mekanisme antiproliferatif nanopartikel dalam sel A431 diselidiki dengan pewarnaan *annexin*-FITC/propidium iodida (PI) dan analisis kitaran sel DNA dengan menggunakan sitometri aliran. Tingkat spesies oksigen reaktif (ROS) intrasel diukur dengan menggunakan kit yang boleh didapati secara komersial. Ekspresi apoptosis dan protein berkaitan kitaran sel ditentukan oleh serap Western. Keputusan TEM dan SEM menunjukkan bahawa nanopartikel berbentuk sfera dengan taburan saiz partikel tertinggi adalah 11 ke 14 nm, manakala purata saiz hidrodinamik 61.21 ±3.96 nm dan nilai keupayaan zeta ialah -18.67 ±3.12 mV yang diukur oleh DLS. Selain itu, pola XRD menunjukkan bahawa logam Ag mempunyai struktur kubus berpusatkan muka dengan nilai puncak belauan pada 2θ

yang bersudut 38.11°, 44.26°, 64.29°, dan 77.07° sepadan dengan satah kekisi yang masing-masing di (111), (200), (220) dan (311). Keputusan FTIR mendedahkan kehadiran kumpulan berfungsi –OH, C=C dan C-O yang mungkin merupakan agen penstabil dan penukupan. Nanopartikel merencatkan pertumbuhan sel A431 dengan nilai IC_{50} sebanyak 39.58 μg/mL selepas 72 jam rawatan. Sementara itu, nilai IC_{50} untuk ekstrak sendiri dan komersial AgNP ialah 164.3 ug/ml dan 16.89 ug/ml. Penyelidikan lebih lanjut menunjukkan bahawa nanopartikel mencetuskan apoptosis dan kitaran sel terhenti pada fasa S dalam sel kanser A431. Analisis serap Western mendedahkan bahawa *A. angustiloba*-AgNPs menyusutkan ekspresi Bcl-2 tetapi meningkatkan ekspresi kaspase terbelah-3, 9 dan Bax. Tambahan pula, pengawalaturan bawah protein E siklin menunjukkan progressi terjejas dalam fasa S kitaran sel. Ringkasnya, *A. angustiloba*-AgNPs merencatkan pengembangbiakan sel dan menggalakkan apoptosis dalam sel kanser A431 melalui peningkatan pengeluaran ROS intrasel dan mengaktifkan laluan apoptosis yang bergantung pada kaspase dan kitaran sel terhenti. Dapatan awal ini memberikan pemahaman bahawa *A. angustiloba*-AgNPs mempunyai keupayaan antineoplastik yang tinggi, oleh itu, kajian farmakologi yang lebih lanjut perlu dijalankan untuk menyingkap potensinya sebagai agen antikanser.

INVESTIGATION ON ANTIPROLIFERATIVE MECHANISMS OF *ALSTONIA ANGUSTILOBA*- SILVER NANOPARTICLES IN SKIN SQUAMOUS CELL CARCINOMA

ABSTRACT

Traditional methods of nanoparticles synthesis frequently use toxics chemicals and substantial energy, which may have detrimental effects on the environment and human health. Recently, plant-based synthesis of nanoparticles (AgNPs) has emerged as a promising green synthesis method. Herein, we reported the green synthesis of AgNPs using the aqueous extract of *A. angustiloba* leaves and assessed its antiproliferative mechanisms. Initially, the physiochemical properties of *A. angustiloba*-AgNPs were characterised using UV–Vis spectrophotometry, FT-IR, FESEM, EDX, TEM, XRD and zeta sizer analyses. The cytotoxicity of *A. angustiloba*-AgNPs was examined by MTT assays against the A431 cancer cell line. The morphology of the treated cells was examined using fluorescence microscopy and the antiproliferative mechanisms of the nanoparticles in A431 cells were investigated by annexin-FITC/propidium iodide (PI) staining and DNA cell cycle analysis using flow cytometry. The intracellular ROS levels were measured using a commercially available kit. The expression of apoptosis and cell cycle-related proteins was determined by Western blotting. The results of SEM and TEM revealed that the nanoparticles showed a spherical shape with the highest particle size distribution was 11 to 14 nm, while a mean hydrodynamic size of 61.21 ±3.96 nm and a zeta potential value of –18.67 ±3.12 mV that was measured by DLS. Besides that, the XRD pattern showed that metallic Ag has a face-centred cubic structure with the diffraction peak values at 2θ of 38.11°, 44.26°, 64.29°, and 77.07°

corresponding to lattice planes at (111), (200), (220), and (311), respectively. FTIR results revealed the presence of –OH, C=C and C-O may serve as a capping and stabilising agent. The nanoparticles inhibited the growth of A431 cells with an IC_{50} value of 39.58 μg/mL after 72 h of treatment. Meanwhile, the IC_{50} values for extract alone and commercial AgNPs were 164.3 ug/ml and 16.89 ug/ml, respectively. Further investigation has shown that the nanoparticles induced both apoptosis and cell cycle arrest at S-phase in A431 cancer cells. Western blotting analysis revealed that *A. angustiloba*-AgNPs decreased the expression of Bcl-2 while increasing the expression of cleaved caspase-3, 9 and Bax. Moreover, the downregulation of cyclin E protein indicated impaired progression in the S phase of the cell cycle. In summary, *A. angustiloba*-AgNPs inhibit cell proliferation and promote apoptosis in A431 cancer cells through increasing intracellular ROS production and activating the caspase-dependent apoptotic pathway and cell cycle arresting. These preliminary findings provided an insight that *A. angustiloba*-AgNPs have high anti-neoplastic potential, therefore further pharmacological studies should be conducted to unveil its attractiveness as an anticancer agent.

CHAPTER 1

INTRODUCTION

1.1 Research background

1.1.1 Green synthesis in nanotechnology and its challenges

Nanotechnology refers to the sophisticated processes, technologies, and techniques to manipulate molecular particles at nano-scale levels, specifically within the range of 1–100 nm (Makhlouf & Barhoum, 2018). Consumer products produced based on nanotechnology facilitate humans to revolutionise their ways of life, especially in novel drug development, material construction, and technical instruments. Nanotechnology contributes to developing nano-electronic biosensors, drug delivery, molecular nanotechnology, and nanomaterials in the medical field. The application of nanotechnology provides the knowledge and appropriate research tools to manipulate modern nano-scale medicinal materials, improving medical and healthcare qualities through accurate therapy and diagnosis with observance of regulatory and safety issues (Alshahrani, 2016).

The global research community has constantly engaged in developing non-toxic, ecologically friendly, and highly effective nanoparticles through green nanotechnology and biotechnology approaches. Green synthesis, which is also referred to as biological synthesis, exploits the living organisms and their biological components, such as fungi, bacteria, algae, plant extracts, and living plants, as the main precursors to produce environmentally amiable nanoparticles (Küünal, Rauwel & Rauwel, 2018). Since the constituents found in the plant or microorganism serve as stabilising and capping agents of nanoparticles, it is needless to supplement external stabilising and capping agents in the synthesis process (Makarov *et al.*, 2006).

The green synthesis of metal oxide or metal nanoparticles involves the use of plant components, which are usually extracted from various plant parts, such as the seeds, fruit peel, latex, tuber, bark powder, leaf, stem, fruit and root (Küünal, Rauwel & Rauwel, 2018). The presence of myriad metabolites and reductive biomolecules in plant extracts, such as amino acids, proteins, vitamins and organic acids, as well as secondary metabolites, including heterocyclic compounds, alkaloids, flavonoids, polyphenols, terpenoids, ketones, aldehydes, amides, and polysaccharides, are responsible for the fast reduction of metal salt from positive oxidation (metal state) to zero oxidation state (nanoparticles) but also serve as the capping and stabilising components in the process (Roy *et al.*, 2019; Duan *et al.*, 2015). Moreover, plant extracts are essential for controlling the size distribution of metallic nanoparticles since the rapid reaction rate may generate smaller nanoparticles and prevent aggregation (Roy *et al.*, 2019).

Although there are many prospects for green nanomaterial synthesis, there are difficulties with raw material selection, reaction conditions, product quality control, and applicability. Moreover, using raw materials can be challenging in real-world production due to time constraints. For example, cotton leaves are ideal for synthesizing silver nanoparticles (AgNPs) only during the flowering season. Trees of Arabica can take around seven years to mature completely and are typically planted at an altitude of 1,500 metres. Various green synthesis methods require high temperatures and prolonged periods of synthesising, which can result in energy consumption that can harm the environment. The process often fails to follow sustainable synthesis principles even though it uses eco-friendly starting ingredients (Pal, Chakroborty & Nath, 2022).

1.1.2 Drawbacks from the chemical and physical synthesis of nanoparticles

The synthesis and stabilisation of nanoparticles have been achieved through conventional approaches, such as physical and chemical synthesis. Physical synthesis methods include high-energy radiation, lithography, and laser ablation, whereas chemical synthesis methods involve photochemical reduction, electrochemistry, and chemical reduction. Despite their practical use over the past two decades, among the components in conventional chemical synthesis are toxic substances with potential risk hazards, such as stabilisers, organic solvents and reducing agents. These substances contribute to severe carcinogenicity, environmental pollution, and cytotoxicity (Ai *et al.*, 2011).

For instance, the chemical synthesis of AgNPs includes mixing a reducing agent (borohydride), a capping agent (starch, polyethene glycol), and other stabilising agents. However, the presence of harmful and hazardous agents in the nanoparticles mixture has led to the banning of the chemical synthesis method of AgNPs in the clinical and biomedical fields (Kulkarni and Muddapur, 2014; Jain *et al*., 2011).

In terms of the physical approaches, the synthesis of nanoparticles is mainly based on a top-down strategy without incorporating any harmful solvent and less waste. Generally, physical synthesis methods produce uniform and monodisperse nanoparticles by several methods, such as electrical energy, thermal energy, high-energy radiations, and mechanical pressure to stimulate evaporation, condensation, abrasion or melting (Dhand *et al.*, 2015).

However, the physical synthesis approach is uneconomical due to its high-energy requirement, which generates extreme heat and elevates the temperature surrounding the source materials. Besides, the method is time-consuming based on the need to achieve thermal stability. For instance, a typical tube furnace requires at least several kilowatts of electricity to produce nanoparticles with a preheating time of several minutes to stabilise the operating temperature (Iravani *et al.*, 2014).

Furthermore, the standard operation of conventional physical synthesis methods, which is based on the principle of pressurised gases and vacuum coupled with high temperatures requires advanced and expensive instrumentations (Shah *et al.*, 2015). By contrast, green-based synthesis methods have overcome these limitations by excluding the use of reducing, capping, or reducing agents.

1.1.3 Global incidence and mortality of cancers and skin cancer

The cancer rate in low-income countries is relatively high due to delayed diagnosis, which implies that the patients would only seek medical treatment when the cancer has advanced to the incurable or metastatic stage. According to the estimates by the International Agency for Research on Cancer (IARC), Asia and Africa recorded a higher number of cancer deaths (7.3% and 57.3%, respectively) compared to cancer incidence (5.8% and 48.4%, respectively). The report indicates that Asian countries represent 50% of newly diagnosed cancer cases and 50% of the mortality rate (World Health Organization, 2018).

In Malaysia, approximately 60% of cancer prognosis is only discovered during the later stages of cancer progression. This is due to the lack of awareness among patients and their relatives on the importance of early cancer detection and screening. According to the Malaysia National Cancer Registry Report 2012–2016, the three most-common cancers among men in Malaysia are colorectal (14.8%), lung (13.2%), and prostate (7.7%) cancers, while the highest cancer cases among Malaysian women are breast (34.1%), colorectal (11.1%), and cervix (6.2%) cancers (Manan *et al.*, 2019).

Table 1.1 Ten most common cancers among Malaysian residents from 2012 until 2016. Breast cancer is the highest cancer case (Source: Manan *et al.*, 2019).

ICD-10	Sites	No.	%
C50	Breast	21,925	19
C18-21	Colorectal	15,515	13.5
C33-34	Trachea, bronchus and lung	11,256	9.8
C81-85, C96	Lymphoma	5,830	5.1
C11	Nasopharynx	4,597	4.0
C91-95	Leukaemia	4,273	3.7
C61	Prostate	4,189	3.6
C22	Liver	4,033	3.5
C53	Cervix uteri	3,981	3.5
C56	Ovary	3,575	3.1
	Others	36,064	31.3
	Total	**115,238**	**100.0**

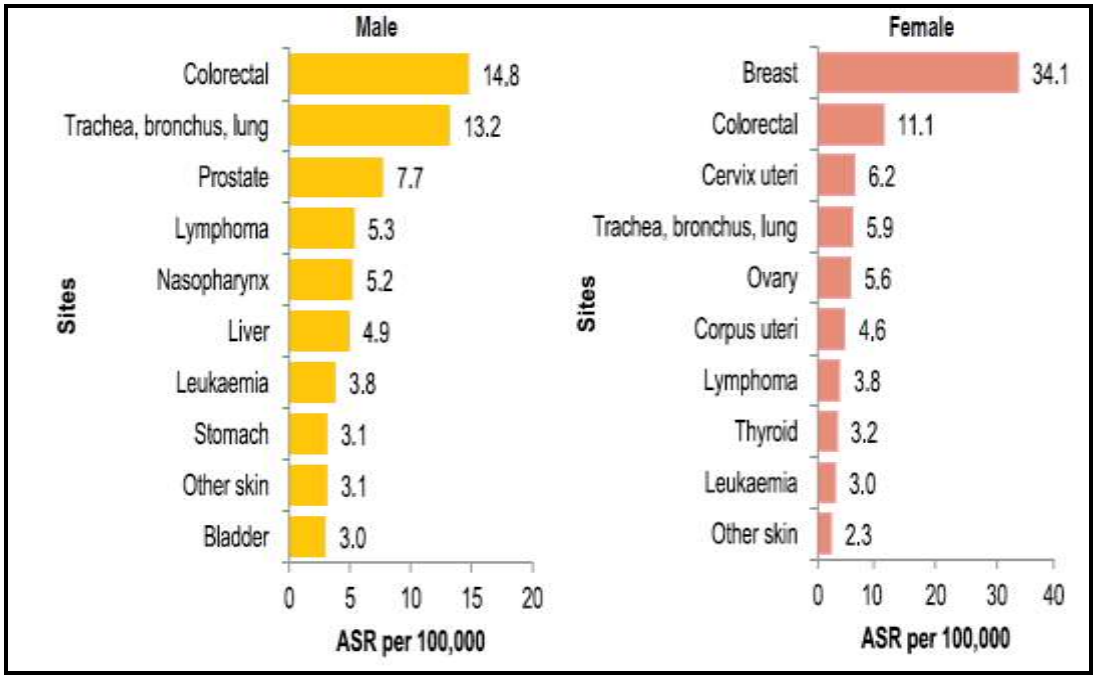

Figure 1.1 Age-standardised incidence rates according to the sex for Malaysia's most frequent ten cancers from 2012 until 2016. Other skin refers to non-melanoma skin cancer (NMSC). NMSC is the ninth most prevalent cancer for males and the tenth most common cancer for females (Source: Manan *et al.*, 2019).

The study was focused on skin cancer due to its incidence and prevalence, as it rises rapidly annually. This condition has a significant impact on public health. The global disease burden of non-melanoma skin cancer (NMSC) is alarming. It shows that the disease seriously threatens human health (Hu *et al.*, 2022). Interestingly, every year, the consistent increase in skin cancer has ranked it as one of the most prevalent diseases worldwide. In 2003, the World Health Organisation (WHO) estimated that 2–3 million patients worldwide were diagnosed with skin cancer yearly. The total case consists of 4% melanoma (around 130,000 cancers), 80% basal cell carcinoma (BCC) and 16% cutaneous squamous cell carcinoma (cSCC). In fact, global melanoma cases have increased by 287,723 as of 2018 (Freeman *et al.*, 2020).

While the incidence of melanomas is still considered low, the disease has been associated with causing death since it can spread rapidly to other body parts. Hence, early detection and treatment of melanoma have been shown to improve the five-year survival rate to as high as 91–95% (Freeman *et al.*, 2020). According to the Malaysian National Cancer Registry Report 2012-2016 by the Ministry of Health in 2019, skin cancer is Malaysia's 10th most frequent cancer, accounting for 2.6% of all cancer cases. Between 2012-2016, there were 3192 NMSC cases (incidence 2.6), of which 1797 were males and 1395 were females, with an incidence rate of 2.6 and 2.1 per 100 000 populations, respectively. The total of melanoma cases was about 347, of which 184 in males and 163 in females, with incidence rate of 0.4 and 0.3 per 100 000 populations, respectively (Manan *et al.*, 2019).

Although melanoma is not predominant in Malaysia, the number of patients that had received treatment at a dermatology clinic in Hospital Kuala Lumpur was only about 5.4%. This is due to the lack of awareness among patients on the existence of this type of cancer. In particular, Asian people who are fair-skinned showed three times higher rates of contracting skin cancer than those with darker skin complexion. The finding correlates with the increased prevalence of skin cancer cases in Singapore, especially among older Chinese citizens between 1968 and 2006 (Narayanamurthy *et al.*, 2018). In comparison, an annual increase of 5.4 million new skin cancer cases was recorded in the USA, with approximately 10,000 deaths due to melanoma, which accounted for 75% of all skin-cancer-related deaths in a year (Esteva *et al.*, 2017).

The underlying factors of skin cancer are related to environmental and constitutional aspects. Exposure to UV radiation (UVR) from sunlight is an environmental risk factor that triggers varying effects of skin cancer development. While chronic exposure can lead to cSCC, exposure during childhood and intermittent exposure to UV are closely associated with BCC. Furthermore, constitutional risk factors are usually correlated with genetic susceptibility, eye and hair colour, as well as skin phototypes (Song *et al.*, 2012).

Recently, Affandi (2018) conducted a 13-year retrospective review (from 2005 to 2017) on skin cancer patients who obtained treatments in the Department of Dermatology, Hospital Kuala Lumpur. The study revealed that BCC was the most common type of skin cancer (31.9%), while malignant melanoma (5.6%) was the least common skin cancer. The findings were parallel with the global statistic on skin cancer, which also reported that BCC was the most frequent type of skin cancer. Additionally, the study found that the intermediate cases of cSCC and cutaneous lymphoma were 24.2% and 25.4%, respectively (Affandi, 2018).

Multiple forms of skin cancer are treated with chemotherapy and radiotherapy. Nevertheless, skin cancer cells may resist these treatments due to their highly proliferative potential (Kalal, Upadhya & Pai, 2017). The key factor contributing to chemotherapy resistance is the limited information regarding the suitable amount of drug needed to reach the tumour site and affect the tumour microenvironment. According to a recent study, the phenomenon of drug resistance in skin cancer therapy arises from gene mutations that occur during treatment or from the elevated expression of targeted molecules via the switching of compensatory signaling pathways (Feoktistova & Panayotova-Dimitrova, 2017).

Subsequently, the resistance phenomenon of skin cancer generates chemo-resistant cells that eventually bypass cell death signals through various mechanisms, such as metabolic change, drug efflux, alteration in the repairing mechanism of deoxyribonucleic acid (DNA) damage, and/or other unknown mechanisms (Zhang *et al.*, 2020). Thus, there is an immediate demand to investigate the synthesis or development of novel and less expensive therapeutic entities to battle cancer cells without or with a low risk of acquiring chemo resistance.

1.1.4 The global challenge in the treatment of skin cancer

Currently, surgical excision is considered the first-line therapy and gold standard for non-melanoma skin cancer (NMSC). Past reports have shown that surgical treatment is the most effective treatment for both cSCC and BCC, with over 90% cure rate and more than 95% successful treatment reported for BCC (Lanoue and Goldenberg, 2016; Lewin and Carucci, 2015). However, surgical treatment is strictly forbidden for patients with wound healing problems (Vazquez & Florez-White, 2020).

In addition, there is a chance of complications with surgery, including fatal infections in the elderly, although high cure rates can be attained through operations. Hence, some factors must be considered when dealing with elderly patients, such as their mental health, general state of health, life expectancy, and even their consent to perform the surgery. The availability of other treatment approaches other than surgery should also be carefully selected. For younger patients, Mohs micrographic surgery (MMS) and standard surgical excision are the preferred options to treat NMSC (Čeović *et al.*, 2018).

Apart from surgical treatment, several non-surgical treatments have been proposed, such as radiotherapy, photodynamic therapy (PDT), topical medications, cryotherapy and Hedgehog pathways inhibitors. Nevertheless, each of these methods exhibits specific limitations. Therefore, the best treatment method choice must be made according to the individual's biological behaviour, such as the anatomic site of the tumour, size, and features of histological observations. Other aspects of evaluations should also be considered, including the patient's conditions, such as mental status, comorbidities, and functionality (Čeović *et al.*, 2018).

Table 1.2 Limitations of different treatments of SCC.

Methods	Limitation
Mohs micrographic surgery (MMS) (Brodland & Zitelli, 1992)	It cannot capture micrometastases, time-consuming and costly (Tierney & Hanke, 2009).
Electrodesiccation and curettage (E&C) (Freeman *et al.*, 1964)	It cannot be used for recurrent or high-risk SCC (Reschly & Shenefelt, 2010).
Cryosurgery (Kuflik, 2004)	Not appropriate for locally recurrent disease or high-risk tumours (Almeida Gonçalves, 2011).
Radiotherapy	It cannot be used for verrucous carcinoma (Miller, 2000), produces pallor and telangiectases in treated patients, not suitable for cartilage due to necrosis risk (Inaba *et al.*, 2013).
Photodynamic therapy (Stebbins & Hanke, 2011)	It is restricted to Bowen's disease with well-differentiated lesions and micro-invasive SCC (Kallini, Hamed & Khachemoune, 2015).
Locally applied treatment (topical imiquimod, intralesional interferon-χ (IFN-χ) and tropical 5-FU) ((Bath-Hextall *et al.*, 2013; Lansbury *et al.*, 2010).	Sufficient evidence is lacking (Kallini, Hamed & Khachemoune, 2015).
Systemic chemotherapy with the cytotoxic agent in SCC	Still unclear, not well-established (Deconti, 2012).

Since 2010, the monthly cost of cancer treatment with newly approved drugs has exceeded USD10,000, which is ten times higher than in the previous decade. The higher price of cancer treatment reflects the rising cost of new drug development and suggests modifications in the latest medication used. In addition, antibody-based cancer therapeutics have received approval from the United States Food and Drug Administration (US FDA) since 2010 as an alternative agent for cancer treatment to replace chemotherapeutics, which are not an ideal option due to their association with the development of chemoresistance in tumour cells. After repeated exposure to chemotherapy drugs, tumour cells can develop a defensive mechanism and become invulnerable to chemotherapy (Chitkara, Mittal & Mahato, 2018).

Furthermore, the direct cost of NMSC treatment has surpassed USD1.5 billion as the incidence of malignancy consistently increases yearly (Palyca *et al.*, 2014). In 2013, the total treatment cost for metastatic melanoma was $12,111 per patient/month (PPPM), while the average total and cSCC-specific costs were $ 18,409.05 (±$ 54,890.57) and $ 7,385.82 (±$ 26,863.88) PPPM, respectively. Treatment for more advanced cSCC patients requires a substantially higher cost than other skin cancers' reported treatment costs (Ruiz *et al.*, 2018).

Most advanced cSCC cases can be treated with surgery, and some patients have performed radiation and/or systemic therapy (Ruiz *et al.*, 2018). However, the establishment of standard care for advanced cSCC patients is still insufficient, emphasising the need for further clinical studies for this population. Besides, treating SCC remains a significant challenge due to the potential development of chemoresistance.

Although a variety of therapies for NMSC have been utilised, including 5-fluorouracil, ingenol mebutate, imiquimod and diclofenac, methotrexate, cetuximab, destroy cancer cells because the cells developed resistance to the treatments (Amaral & Garbe, 2017). As the incidence of NMSC persistently increases, the rising surgical treatment cost compared to non-surgical alternatives requires further consideration.

Table 1.3 Summary of resistance mechanisms and NMSC-related chemotherapeutic agents. The agents failed to diminish or eradicate cancer cells.

Cytotoxic agent	Resistance mechanism	References
Methotrexate	Increased activity of drug target	Bertino *et al.*, 1996
	Reduced cellular accumulation	Trippett *et al.*, 1992; Dixon *et al.*, 1994
5-fluorouracil	Inhibition of apoptosis	Liang *et al.*, 2002
	Decreased active metabolite	Beck *et al.*, 1994
Vismodegib	Mutation of Smoothened (SMO) cause reactivation of Hedgehog pathway	Hansel *et al.*, 2015
Cetuximab	Altered functional status of epidermal growth factor receptor (EGFR)	Kjær *et al.*, 2016
	The decrease in EGFR receptor levels	
	Loss of cetuximab binding due to mutations in the extracellular EGFR	

1.2 Relevance of the study

The geographic location of Malaysia at the equator signifies the immense level of solar UVR it receives throughout the year (Tan, Lim & Mat Jafri, 2018). Accordingly, prolonged recreational exposure to sunlight and a history of sunburn are often correlated with the occurrence of skin cancer (Wu *et al.*, 2016). Consequently, skin cancer is Malaysia's 10th most prevalent cancer, accounting for 2.6% of all cancer cases (Manan *et al.*, 2019). The SCC, under the category of NMSC is a common skin cancer type (Demir & Faruk, 2020). Although the varying skin cancers can be treated by chemotherapy and radiotherapy, the highly proliferative potential of skin cancer cells could progressively resist these treatments (Amaral & Garbe, 2017). Thus, developing or synthesising new and cheaper therapeutic agents that offer zero or minimal risk of chemoresistance phenomenon is essential to achieve a greater treatment rate.

Green synthesised plant-based nanoparticles are a proposed therapeutic agent in cancer studies. The diversely available biological entities in the ecosystem provide the necessity to develop advanced biosynthesis procedures over conventional methods. Numerous research on the green biosynthesis of nanoparticles has been successfully demonstrated, providing enormous advantages in different applications, such as diagnosis, treatment, commercial product, and nano-device manufacturing. The utilisation of eco-friendly and green biosynthesis methods can also mitigate the impact of environmental pollution. The plant extract was selected based on the availability of the primary and secondary metabolites, including alkaloids and flavonoids, that are mainly responsible for the sustained redox reaction to reduce ionic structures into metallic nanoparticles (Kuppusamy *et al.*, 2016).

In the present study, *Alstonia angustiloba (A. angustiloba)*, locally known as "Pokok Pulai Bukit", was used to synthesise AgNPs. It is a widely distributed terrestrial plant in Peninsular Malaysia. It was reported that *A. angustiloba* is extensively found in the lowland forests of Sabah and contains bioactive alkaloids that can be extracted from its bark and leaves (Goh *et al.*, 1997). Currently, there are 20 known alkaloids in the bark and stem of *A. angustiloba*, including angustilobine and andranginine. The cytotoxicity of these substances has also been demonstrated in the oral squamous cell carcinoma (KB) cell line (Ku *et al.*, 2011).

Moreover, the various bioactive compounds in *A. angustiloba*, such as bioactive alkaloids (Ku *et al.*, 2011; Goh *et al.*, 1997), flavonoids, and steroids (Zuraida, 2019), have the potential to serve as the reducing and stabilising components for the AgNPs fabrication.

The outputs of this study may allow future studies to investigate the association between nanoparticle properties and their efficiency towards various cancer cell lines. Shape, size, surface chemistry, capping/ coating, composition, reducing agents, type of cell, ion release, reactivity, agglomeration, and dissolution rate for AgNP synthesis are all important factors in determining cytotoxicity. Hence, researchers be able to determine the ideal nanoparticle characteristics that maximise antiproliferative potential by systematically altering these factors (Zhang *et al.*, 2016). Besides that, future studies can concentrate on the mechanobiological characteristics of cells, such as elasticity and adhesion, which are crucial to cellular processes and cancer development. Cellular processes may change due to interactions between nanomaterials and cells, which may also impact the development of cancer (Sohrabi Kashani & Packirisamy, 2021).

Therefore, this study focused on the green synthesis and characterisation of AgNPs (scanning and transmission electron (SEM, TEM), zeta potential, dynamic light scattering (DLS), Fourier transform infrared (FTIR), X-ray diffraction (XRD)) through the reaction between silver nitrate ($AgNO_3$) and aqueous leaves extract of *A. angustiloba* (section 4.1). The leaves extract was then characterised by antioxidant activity, phenolics and flavonoid content, and liquid chromatography-mass spectrometry (LC-MS) that contributed to the green synthesis of AgNPs (section 4.2). The synthesised product was then subjected to cytotoxicity study and morphological changes on skin squamous cell carcinoma (A431) and fibroblast cell (L929) (section 4.3). Moreover, evaluations of cell death mechanism via apoptosis (Annexin V-FITC/PI) and cell cycle arrest were carried out using a commercial kit (section 4.4). Finally, the research investigated the expression of apoptotic and cell cycle protein expression using Western blotting in the A431 cell lines induced by *Alstonia angustiloba*-silver nanoparticles (*A. angustiloba*-AgNPs) (section 4.5).

1.3 Objectives of the study

The main objective of this study is to explore the potential anti-tumour properties and possible mechanisms of green synthesised AgNPs from *A. angustiloba* leaves extract. The specific objectives are as follows:

1. To characterise green synthesised AgNPs from *A. angustiloba* leaves extract.
2. To profile phytochemicals in *A. angustiloba* leaves extract that contribute to the green synthesis of *A. angustiloba*-AgNPs
3. To evaluate the cytotoxicity effect of *A. angustiloba*-AgNPs on target (A431) and non target cells (L929).
4. To determine the cell death mechanism of *A. angustiloba*-AgNPs against the A431 cell line.
5. To identify the expression pattern of proteins in the A431 cell line that responds to the green synthesised AgNPs.

CHAPTER 2

LITERATURE REVIEW

2.1 Skin

2.1.1 Anatomy, histology and pathology

The skin is the largest organ that covers the exterior surface of the whole body of a human. It has three surfaces, namely the epidermis, dermis, and hypodermis, where each layer possesses its distinct anatomy and function (Yousef, Alhajj & Sharma, 2021). Table 2.1 describes the skin's primary functions.

Table 2.1 The primary functions of the skin. It is essential for protection, sensation and regulation.

Functions	Actions
Defensive barrier	Protect the body from microorganism invasion, water, trauma caused by chemical and mechanical agents and damage from UV light ((Greaves, 2007).
Homeostasis balance	Regulate water loss and body temperature (Osilla, Marsidi & Sharma, 2021).
Endocrine and endocrine	Endocrine – With UV light, Vitamin D is made in the keratinocytes. Keratinocytes express vitamin D receptor (VDR) and release enzymes to produce the active form of 1, 25 dihydroxy vitamin D (Yousef, Alhajj & Sharma, 2021). Exocrine – Skin contains sweat and sebaceous glands (Brodell & Rosenthal, 2008).
Sensation	Nociceptors respond to heat, pain, touch and cold (Dubin & Patapoutian, 2010).
Immunological defence	The adaptive immune system is developed by Langerhans cells in the epidermis (dendritic epidermal T lymphocytes) (Yousef, Alhajj & Sharma, 2021).

The top skin layer consists of the epidermis, which has an approximate thickness of 50–100 µm. Figure 2.1 illustrates the various type of cells that forms this layer, primarily keratinocytes, several Langerhans cells, and melanocytes. The stratum corneum is the epidermis's outermost layer, which maintains the integrity of the permeable barrier, as this layer is composed of 20% water, 20% lipids and 60% structural proteins (Farage *et al.*, 2013). This barrier minimizes the passive loss of body water, reduces chemical absorption from the surrounding environment, and protects the skin against microbial infection (Wickett & Visscher, 2006). Additionally, the lipid compositions in this layer, such as ceramides, cholesterol, and fatty acids, are vital for constant skin integrity (Farage *et al.*, 2013).

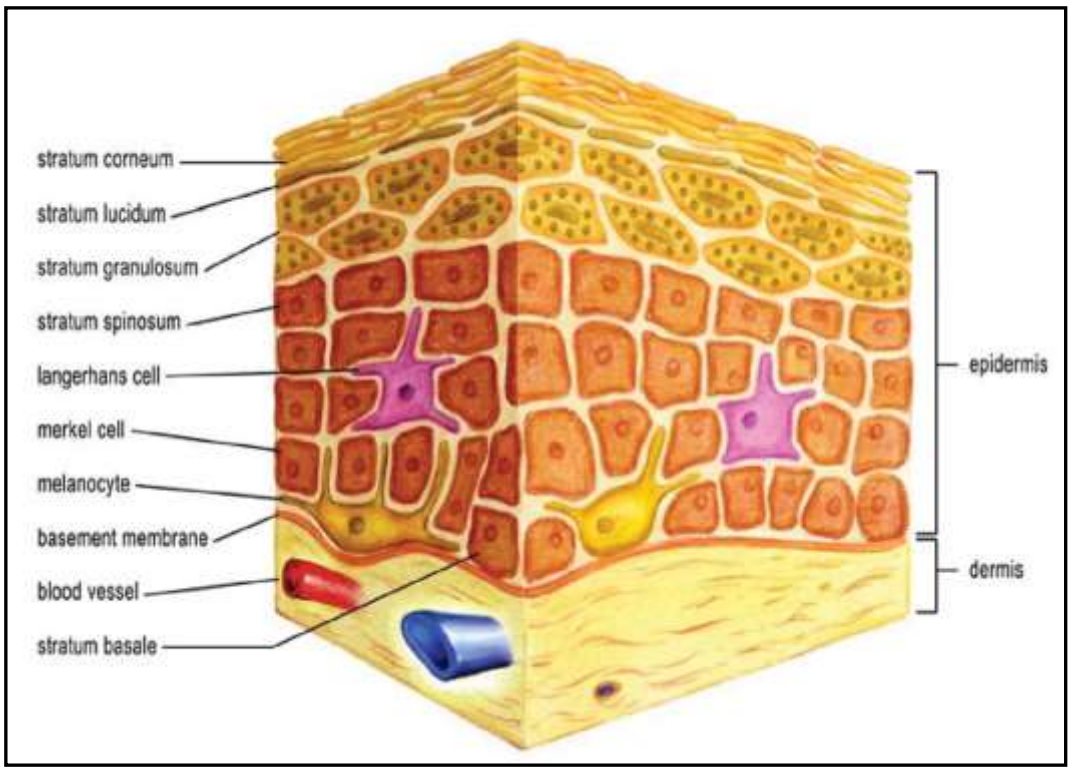

Figure 2.1 Anatomy of normal skin with epidermis and dermis layer. The epidermis is the skin's outermost layer, and the dermis is the thickest layer beneath the epidermis (Source: Farage *et al.*, 2013).

The stratum lucidum is the thick neighbouring layer below the stratum corneum and is usually located in the soles and palms. The cells have an opaque membrane with nucleated and dense cytoplasm. Next, three to four layers of stratum granulosa composed of granules with diamond-shaped cells are located under the stratum lucidum. The granules contain proteins that accumulate the keratin filaments and cells that bind the stratum corneum together. Below the stratum granulosa are four to ten stratum spinosum layers consisting of polyhedral cells. Intracellular bridges are formed between the cells to connect the cells with each other. In addition, the cytoplasm has tonofilaments and a few organelles that form keratin and assist in binding this layer to the stratum corneum. The shape of the cell nucleus is relatively oval (Zaidi & Lanigan, 2010).

The middle skin layer, known as the dermis, is composed of a tough fibrous layer 2–3 mm thick. This layer consists predominantly of blood vessels and connective tissue to sustain the above epidermis layer. Specifically, the collagen fibres in the dermal connective tissue provide the required tensile strength, while the elastin fibres provide resilience and elasticity, which give the skin the recoil property. Elastic fibres can be destructed by prolonged UV light exposure during ageing, consequently leading to wrinkle formation. Meanwhile, blood vessels in the dermis layer play an essential role in maintaining the body temperature and supplying the necessary nutrients to the skin. Other vital components, such as hyaluronic acids, nerve fibres, supportive glycosaminoglycans, and sensory receptors, are also located in the dermis layer (Farage *et al.*, 2013).

Nerve fibres are important to protect us from injury caused by pressure, cold, heat and pain, and cutaneous sensations. The lack of senses can cause leprosy (Zaidi & Lanigan, 2010). The hypodermis is the bottom and skin's innermost layer. It mostly comprises adipocytes organised into lobules separated by fibrous connective tissue (septae). The loose connective tissues then bind this innermost layer to the adjacent internal organs. The nerve, lymphatic and blood vessels are contained in the septa. Additionally, areolar tissue and subcutaneous fat play a role in cushioning, thermoregulation, and stability (Farage *et al.*, 2013). Moreover, the subcutaneous tissue is considered an endocrine organ that converts androstenedione into estrone by the aromatase enzyme (Gilaberte *et al.*, 2016). In short, the hypodermis layer preserves skin integrity, provides a reserve energy source, and facilitates mobility by sliding over the underlying components.

2.1.2 Pathophysiology

Skin diseases are categorised into two groups according to their etiological factors: proliferative/neoplastic and inflammatory/infectious. Proliferative conditions include seborrheic keratosis, psoriasis cysts, warts, and papillomas. At the same time, benign tumours include hemangiomas, lipomas, dermatofibromas, nevi, and neuromas. Examples of malignant tumours are Kaposi sarcoma, melanoma, and NMSC (Banasik, 2018). In contrast, inflammatory skin diseases usually occur among individuals with triggered hypersensitivity reactions from environmental substances (Weller *et al.*, 2014; Farage *et al.*, 2013). Being the outermost layer of the human body, the skin is exposed to various infectious organisms, ranging from viruses to insects (Vollono *et al.*, 2019).

The primary and secondary lesions can be used to identify the type of skin disease based on the description of the skin lesion, including its shape, number, and colour. The skin preserves its original structure for primary lesions and is unaffected by time or external factors, such as scratching. These include non-palpable, solid, and fluid-filled palpable lesions. However, the appearance of secondary lesions is not the same as the primary lesions, where the skin structure is damaged and affected as a result of alterations over time (Banasik, 2018). Secondary lesions can be divided into diminished or damaged skin surface and increased or augmented skin surface.

2.2 Cancer

2.2.1 Incidence

Cancer disease is a self-sustaining and dynamic adaptation process through interaction with the surrounding microenvironment (Quail & Joyce, 2013). Despite substantial progress in cancer research, the complexity of each cancer stage management presents an unremitting challenge to patients, researchers, and clinicians.

With almost one over six deaths worldwide, severe metabolic syndrome in cancer is the second most deadly illness after cardiovascular disease (Ritchie & Roser, 2018). In fact, the WHO reported that in 2015, cancer was the first or second leading cause of death in 91 out of 172 countries for populations aged less than 70 years. Meanwhile, it was ranked third or fourth on the death chart in 22 other countries (Bray *et al.*, 2018). Evidently, cancer cases are steadily rising annually, with an estimated count of nearly 21 million cancer patients by 2030 (Iqbal *et al.*, 2017). The increasing trend of the global cancer burden is correlated with several factors, such as the prolonged ageing population and the current lifestyle changes linked to rapid socio-economic development (Ferlay *et al.*, 2019). Moreover, the mortality rate and incidence of cancer vary substantially among various countries, corresponding to the different socio-economic statuses and associated lifestyle factors within the society (Subha, 2019).

Figure 2.2 depicts the combined or separated data of the global estimation of cancer cases and deaths in 2020 between males and females. The highest diagnosed cancers among the combined sexes were female breast cancer (11.7%), followed by lung (11.4%), colorectal (10.0%), prostate (7.3%), stomach (5.6%), liver (4.7%), and bladder cancer (3.0%), while the leading cancer death is lung cancer (18.0%), followed by colorectal (9.4%) and liver (8.3%). For males only, lung cancer is the most commonly diagnosed cancer (14.3%), followed by prostate (14.1%) and colorectal cancers (10.6%) (Sung *et al.*, 2021).

Over a hundred different types of cancers can be developed, each with its distinct behaviour and responses to treatment since any type of body cell can undergo abnormal cell proliferation and cause cancer. In cancer pathology studies, a tumour is classified into two types, namely benign and malignant. Normally, cancers are referred to as malignant tumours only if they invade the adjacent healthy tissue and metastasize or disseminate via the circulatory or lymphatic systems throughout the body. Furthermore, a malignant tumour can resist localised treatment approaches once it spreads to a distant body site. Oppositely, a benign tumour, like a typical skin wart, persists in the exact location of its original sites, neither infiltrating adjacent normal tissue nor spreading to distant bodily regions and thus can be easily cut out via surgical methods (Cooper, 2000).

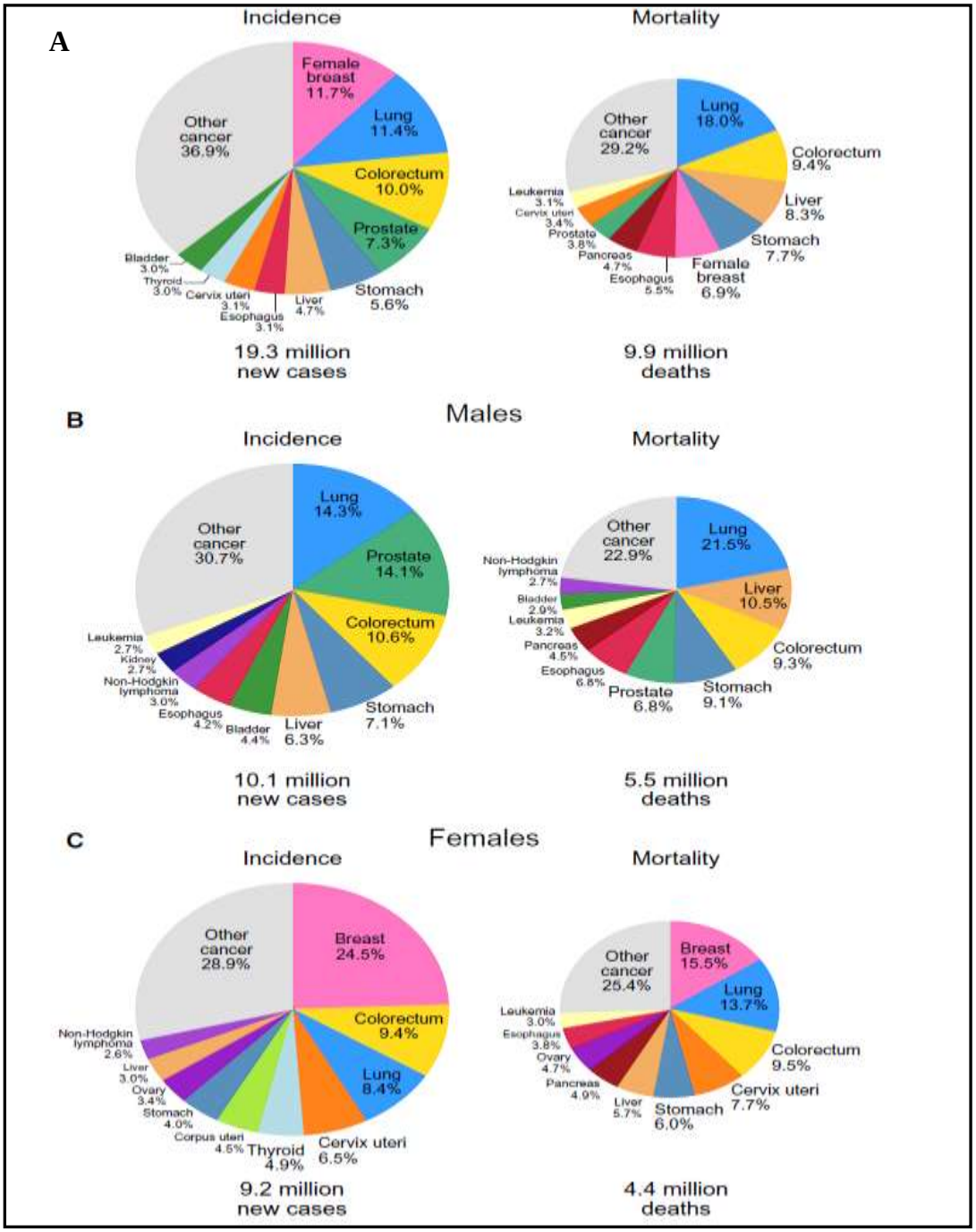

Figure 2.2 The proportion of cases and fatalities for the top ten cancer types in 2020 for (A) both sexes; (B) males and (C) females. The percentage of total cases or fatalities is indicated in each chart; non-melanoma skin cancers (NMSC) are included in the "other" cancer. Source: GLOBOCAN 2020 (Sung *et al.*, 2021).